

# NSun2-Mediated Cytosine-5 Methylation of Vault Noncoding RNA Determines Its Processing into Regulatory Small RNAs

Shobbir Hussain,<sup>1</sup> Abdulrahim A. Sajini,<sup>1</sup> Sandra Blanco,<sup>1</sup> Sabine Dietmann,<sup>1</sup> Patrick Lombard,<sup>1</sup> Yoichiro Sugimoto,<sup>2</sup> Maike Paramor,<sup>1</sup> Joseph G. Gleeson,<sup>3</sup> Duncan T. Odom,<sup>4</sup> Jernej Ule,<sup>2,5,\*</sup> and Michaela Frye<sup>1,\*</sup>

<sup>1</sup>Wellcome Trust – Medical Research Council Cambridge Stem Cell Institute, University of Cambridge, Tennis Court Road, Cambridge, CB2 1QR, UK

<sup>2</sup>Medical Research Council Laboratory of Molecular Biology, Hills Road, Cambridge CB2 0QH, UK

<sup>3</sup>Howard Hughes Medical Institute, University of California, San Diego School of Medicine, La Jolla, CA 92093, USA

<sup>4</sup>University of Cambridge, CR-UK, Cambridge Institute, Li Ka Shing Centre, Robinson Way, Cambridge CB2 0RE, UK

<sup>5</sup>Department of Molecular Neuroscience, UCL Institute of Neurology, Queen Square, London WC1N 3BG, UK

\*Correspondence: [j.ule@ucl.ac.uk](mailto:j.ule@ucl.ac.uk) (J.U.), [mf364@cam.ac.uk](mailto:mf364@cam.ac.uk) (M.F.)

<http://dx.doi.org/10.1016/j.celrep.2013.06.029>

This is an open-access article distributed under the terms of the Creative Commons Attribution-NonCommercial-No Derivative Works License, which permits non-commercial use, distribution, and reproduction in any medium, provided the original author and source are credited.

## SUMMARY

Autosomal-recessive loss of the *NSUN2* gene has been identified as a causative link to intellectual disability disorders in humans. NSun2 is an RNA methyltransferase modifying cytosine-5 in transfer RNAs (tRNAs), yet the identification of cytosine methylation in other RNA species has been hampered by the lack of sensitive and reliable molecular techniques. Here, we describe miCLIP as an additional approach for identifying RNA methylation sites in transcriptomes. miCLIP is a customized version of the individual-nucleotide-resolution crosslinking and immunoprecipitation (iCLIP) method. We confirm site-specific methylation in tRNAs and additional messenger and noncoding RNAs (ncRNAs). Among these, vault ncRNAs contained six NSun2-methylated cytosines, three of which were confirmed by RNA bisulfite sequencing. Using patient cells lacking the NSun2 protein, we further show that loss of cytosine-5 methylation in vault RNAs causes aberrant processing into Argonaute-associated small RNA fragments that can function as microRNAs. Thus, impaired processing of vault ncRNA may contribute to the etiology of NSun2-deficiency human disorders.

## INTRODUCTION

Cytosine-5 methylation (m<sup>5</sup>C) is a common epigenetic modification found in DNA with important regulatory roles in transcription (Suzuki and Bird, 2008). The cellular and molecular functions of m<sup>5</sup>C-modified nucleobases in RNA, however, remain largely unknown. Dnmt2 and NSun2 are currently the only known m<sup>5</sup>C

RNA methyltransferases in higher eukaryotes, and transfer RNA (tRNA) is the confirmed target substrate for both enzymes (Brzezicha et al., 2006; Goll et al., 2006). The regulatory functions of m<sup>5</sup>C modifications in tRNA are not fully understood but have been reported to regulate tRNA stability and cleavage (Schaefer et al., 2010; Tuorto et al., 2012). Deletion of Dnmt2 or NSun2 in yeast, flies, and mice impairs cellular differentiation pathways in skin, testes, and brain (Blanco et al., 2011; Hussain et al., 2013; Rai et al., 2007; Tuorto et al., 2012). In humans, mutations in the *NSUN2* gene can cause disorders that are associated with intellectual disability (Abbasi-Moheb et al., 2012; Khan et al., 2012; Martinez et al., 2012).

Although NSun2-dependent deposition of m<sup>5</sup>C into tRNAs has been widely confirmed, global identification of m<sup>5</sup>C in RNA has been hampered by the lack of suitable molecular techniques. Recent high-throughput RNA methylation profiling by bisulfite sequencing and the chemical modification of cytosine-5 by 5-azacytidine increased the repertoire of RNAs carrying m<sup>5</sup>C modifications (Khoddami and Cairns, 2013; Squires et al., 2012). In this report, we combine various transcriptome-wide methodologies to identify NSun2-specific RNA methylation sites independent of any chemical modification of RNA. CLIP (cross-linking immunoprecipitation) is a stringent technique devised to identify RNA-protein interactions and uses UV crosslinking to induce a covalent bond between protein and RNA (Ule et al., 2003). Combined with next-generation sequencing, the iCLIP protocol enables genome-wide analysis of crosslink sites at nucleotide resolution (iCLIP) (König et al., 2010).

We modified the iCLIP protocol to identify additional RNA methylation targets of NSun2 and termed it miCLIP (methylation iCLIP). In addition to the established tRNA target substrates of NSun2, miCLIP identified coding RNAs and noncoding RNAs (ncRNAs). We establish vault ncRNAs as NSun2-specific methylated targets and confirm the deposition of m<sup>5</sup>C by RNA bisulfite sequencing. Finally, we provide evidence that m<sup>5</sup>C controls the processing of vault ncRNAs into small regulatory RNAs with microRNA functions.

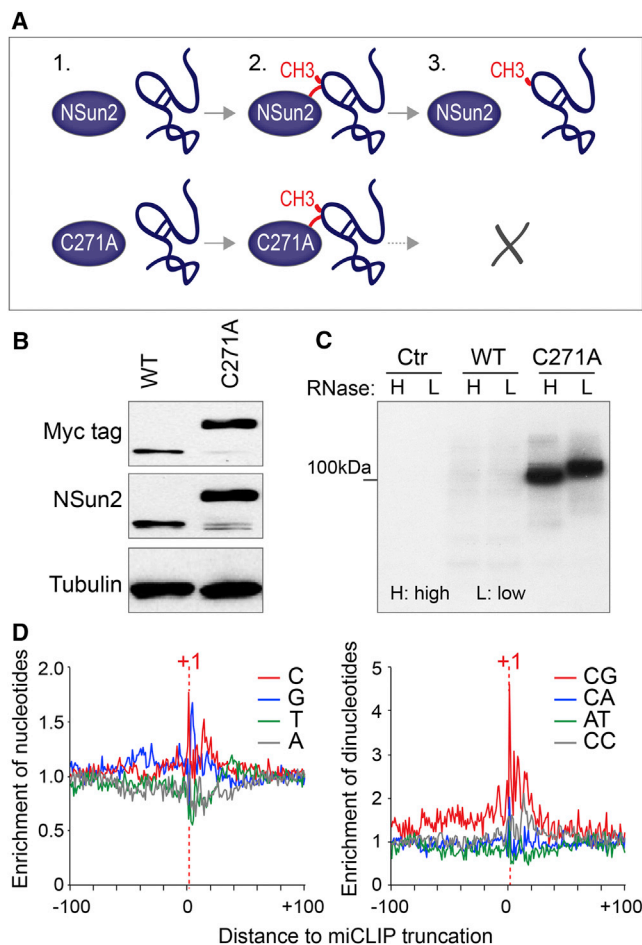


**Figure 1. miCLIP Identifies Cytosine-5-Methylated Nucleosides**

(A) Schematics of NSun2-mediated cytosine-5 methylation and how the C271A mutation causes irreversible covalent crosslinks between the protein and substrate.

(B) Western blot detecting wild-type (WT) and mutant (C271A) NSun2 proteins using an antibody for the Myc tag (top) or NSun2 (middle). Tubulin (bottom) serves as a loading control.

(C) Detection of radiolabeled immunoprecipitated protein-RNA complexes ( $^{32}$ P-ATP) after transfection of an empty vector control (Ctr), wild-type NSun2 (WT), or mutant NSun2 (C271A) using a Myc antibody. Lysates were incubated with high (H) or low (L) concentration of RNase.

(D) Enrichment of nucleotides (left) and dinucleotides (right) in the region up to 100 nt around all crosslink sites. Only the top 4 dinucleotides at position +1 are shown (see also Table S1). See also Figure S1.

## RESULTS

### miCLIP: A Technique to Identify $m^5C$ in the Transcriptome at Nucleotide Resolution

Cytosine methylation at carbon 5 ( $m^5C$ ) is initiated by the formation of a covalent bond between cysteine 321 of NSun2 and the cytosine pyrimidine ring (Figure 1A) (Liu and Santi, 2000). The release of the methylated RNA depends on a second conserved cysteine at position 271 (C271) (Figure 1A) (King and Redman, 2002; Redman, 2006). Mutation of C271 (C271A) stabilizes the

covalently linked protein-RNA catalytic intermediate, which can be detected as higher-molecular-weight complexes by western blot (Figures 1A and 1B) (Hussain et al., 2009).

Because the formation of the protein-RNA covalent bond allowed direct immunoprecipitation of the Myc-tagged C271A NSun2 without UV crosslinking, we named our method miCLIP (methylation iCLIP). The protein-RNA complex was detected by radiolabeling, and a shift in molecular weight in response to a high concentration of RNase I confirmed the presence of the NSun2-RNA complex (Figure 1C). We extracted the RNA from the purified complex and amplified the libraries for 25 or 35 PCR cycles, followed by high-throughput sequencing (Figures S1A and S1B) (König et al., 2010; Sugimoto et al., 2012). We used at least three independent replicates per cell line for all analyses. Analyses of the complementary DNA libraries showed strong cytosine enrichment at position +1 (Figure 1D, left panel), which corresponds to the first nucleotide of all sequence reads (Sugimoto et al., 2012). Thus, reverse transcription terminates precisely at the polypeptide-nucleotide (C271A-cytosine-5) crosslink site. We further detected enrichment of CG dinucleotide at position +1, indicating that deposition of  $m^5C$  occurs preferably at this dinucleotide (Figure 1D, right; Table S1).

### miCLIP-Identified NSun2 Targets Are tRNAs, mRNAs, and ncRNAs

The vast majority of miCLIP reads (>80%) mapped to tRNAs (Figures 2A and 2B). RNA bisulfite conversion identified tRNA Asp<sup>GTC</sup>, Val<sup>AAC</sup>, Gly<sup>GCC</sup>, and Leu<sup>CAA</sup> as methylation substrates of NSun2 in mouse (Tuorto et al., 2012), and miCLIP precisely mapped the expected  $m^5C$  sites in these tRNAs (Figure 2A; Figure S2A). When all tRNA reads were mapped, miCLIP identified a total of 41 isoacceptors (Figure S2B). These results are in good agreement with the recently developed 5-azacytidine-mediated RNA immunoprecipitation method (Aza-IP), where the majority of tRNAs were found to be methylated by NSun2 (Khoddami and Cairns, 2013). miCLIP consistently detected NSun2-targeted sites within the variable arm at cytosines 48, 49, and 50 (Figure S2B). However, it does not detect any additional NSun2 target sites outside the variable arm (Khoddami and Cairns, 2013).

The specificity of the interaction between the C271A mutant protein and its target RNA was further confirmed by the very low number of reads mapped to ribosomal RNAs (rRNAs) (Figure 2B). The total number of reads mapping to other ncRNAs and messenger RNAs (mRNA) was consistently less than 20% (Figure 2C; Table S2). It has been recently suggested that NSun2-mediated methylation of mRNAs may increase their half-life (Zhang et al., 2012); yet gene expression assays in various tissues including testis and liver failed to uncover any major changes in mRNA abundance when NSun2 was deleted (Hussain et al., 2013; Tuorto et al., 2012). The only mRNA identified by miCLIP that was differentially expressed when NSun2 was inhibited by RNAi in HEK293 cells was NSun2 itself (Figure S3A; Table S3). We also sequenced cDNA from total RNA isolated from human skin fibroblasts carrying a heterozygous or homozygous loss-of-function mutation in the *NSUN2* gene (Figure S3B; Table S4) (Martinez et al., 2012). The vast majority of the 312 miCLIP-identified mRNAs (>90%) remained

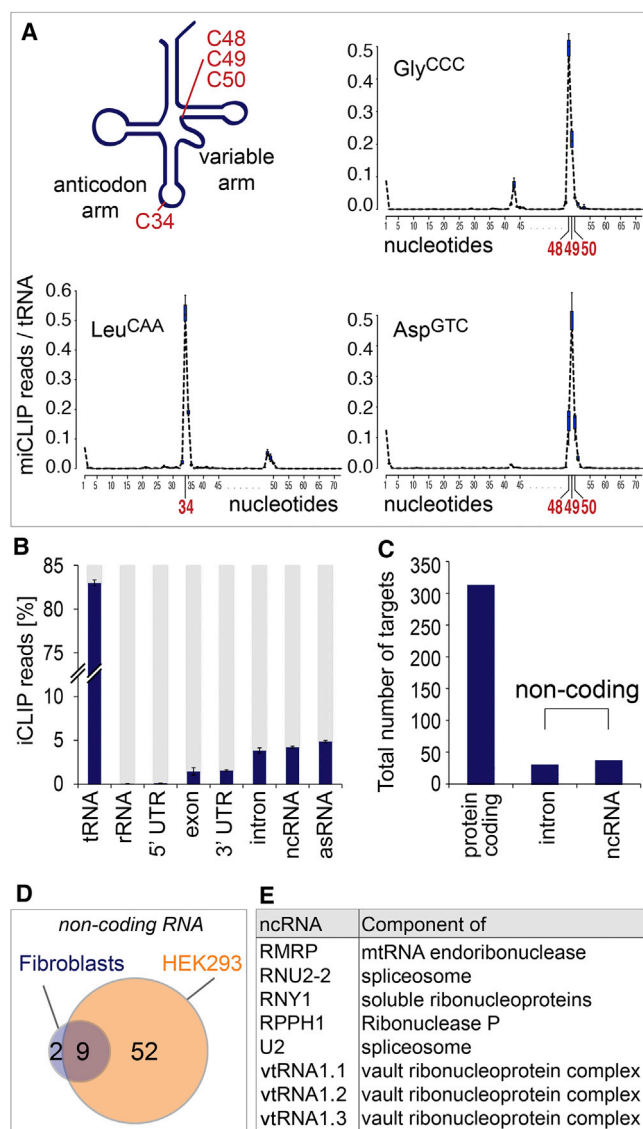


**Figure 2. Detection of Coding and Noncoding RNA by miCLIP**

(A) Schematics of tRNA carrying m<sup>5</sup>C at positions 48, 49, and 50 in the variable arm or at position 34 in the anticodon arm (top left). Frequency of miCLIP reads per tRNA identifies all cytosine-5 methylated sites in tRNA Gly<sup>CCC</sup>, Leu<sup>CAA</sup>, and Asp<sup>GTC</sup> (top right and bottom). See also Figure S2.

(B) Percentage of miCLIP reads in noncoding (tRNA, rRNA, 5' and 3' UTR, intron, ncRNA, and asRNA) and protein-coding RNAs. Shown are common miCLIP targets of three replicates after 25 cycles of amplification. Error estimates represent SD of the mean. See also Figure S2.

(C) Total number of protein-coding, intron, and other noncoding RNAs (ncRNAs) in three replicates after 35 cycles of amplification. See also Figure S3.

(D) Venn diagram of common miCLIP-identified ncRNAs in HEK293 (orange) and human fibroblasts (blue). See also Figure S3.

(E) Description of eight ncRNAs with differential abundance in human fibroblast carrying a heterozygous (+/-) or homozygous (-/-) loss-of-function mutation for *NSUN2*.

unchanged in the absence of NSun2 (Figure S3B). In conclusion, we do not find evidence for a major role of NSun2 or NSun2-mediated m<sup>5</sup>C in mRNA stability.

### NSUN2 Methylates Several ncRNAs

In addition to the tRNAs, miCLIP identified several other ncRNAs. Most of these ncRNAs were identified in both cell types and under both PCR amplification conditions (Figure 2D; Figure S3C). Although the number of ncRNAs found in *NSUN2*<sup>+/-</sup> human fibroblasts was low, they largely overlapped with those identified in HEK293 cells (Figure 2D; Table S2). miCLIP identified a maximum of 61 common ncRNAs, out of which only 43 were annotated (Table S5). We sequenced cDNA libraries prepared from small RNA isolated from *NSUN2*<sup>+/-</sup> and *NSUN2*<sup>-/-</sup> human fibroblasts and found eight of the ncRNAs differentially regulated (Figure 2E; Table S6; Figures S3D and S3F). For instance, miCLIP identified NSun2-target cytosine 174 in RPPH1 and cytosine 92 in 5S rRNA (Figures 3A and 3B; Figure S4A), which agrees with previous RNA bisulfite sequencing and Aza-IP in HeLa cells, respectively (Khoddami and Cairns, 2013; Squires et al., 2012). Additionally, we identified NSun2 target sites in 7SK and the three vault RNAs (vtRNAs) (vtRNA1.1, vtRNA1.2, and vtRNA1.3) (Figures 2E, 3A, and 3C; Figure S4B). Of these, only cytosine 69 in vtRNA1.1 has previously been reported to be methylated by NSun2 using Aza-IP and RNA bisulfite sequencing (Khoddami and Cairns, 2013; Squires et al., 2012).

Vault ncRNAs were first described as components of macromolecular ribonucleoprotein complexes termed vaults, which are conserved organelles found in most species (Kedersha et al., 1990; Kedersha and Rome, 1986). The function of vaults is unknown, yet they have been associated with resistance to chemotherapy in cancer (Mossink et al., 2003). Although vtRNA1.1 is expressed at lower levels than vtRNA1.2 and vtRNA1.3 in HEK293 cells (Stadler et al., 2009), it was the most prominent target identified by miCLIP (Figure 3A). vtRNA1.1 showed a methylated site at C69 and vtRNA1.2 and vtRNA1.3 at C59 (Figure 3C). vtRNA1.2 and vtRNA1.3 shared methylation sites at C27 and C59, and only vtRNA1.3 was additionally methylated at C15 (Figure 3C).

To confirm the NSun2-mediated methylation sites independently, we performed RNA bisulfite sequencing in *NSUN2*<sup>+/-</sup> and *NSUN2*<sup>-/-</sup> human fibroblasts. In line with the miCLIP cDNA counts, vtRNA1.1 showed the highest levels of m<sup>5</sup>C at position 69 (Figures 3A and 3D, right panel). We further confirmed m<sup>5</sup>C at C27 and C59 in vtRNA1.3, whereas RNA bisulfite sequencing failed to detect m<sup>5</sup>C in vtRNA1.2 (Figure 3D, left and middle panels; Figures S4C and S4D). All vtRNAs isolated from *NSUN2*<sup>-/-</sup> fibroblasts lacked m<sup>5</sup>C at the corresponding positions (Figure 3D, lower panels). vtRNAs share high sequence homology and the potentially methylated cytosines C15, C27, and C59/69 are present in all three ncRNAs (Figure S5A). Using LocARNA, a tool that simultaneously folds and aligns input RNA sequences (Smith et al., 2010), we predict that all three cytosines are located in vtRNA stem structures but are either unpaired or next to an unpaired nucleoside (Figure 3C; Figures S5A and S5B).

We noted that the consensus sequence for miCLIP target sites in vtRNAs was TCG (Figure 3C). Although this consensus sequence can vary in tRNAs and other RNAs (data not shown), it raises the possibility that NSun2-mediated methylation may have different molecular functions defined by the context of

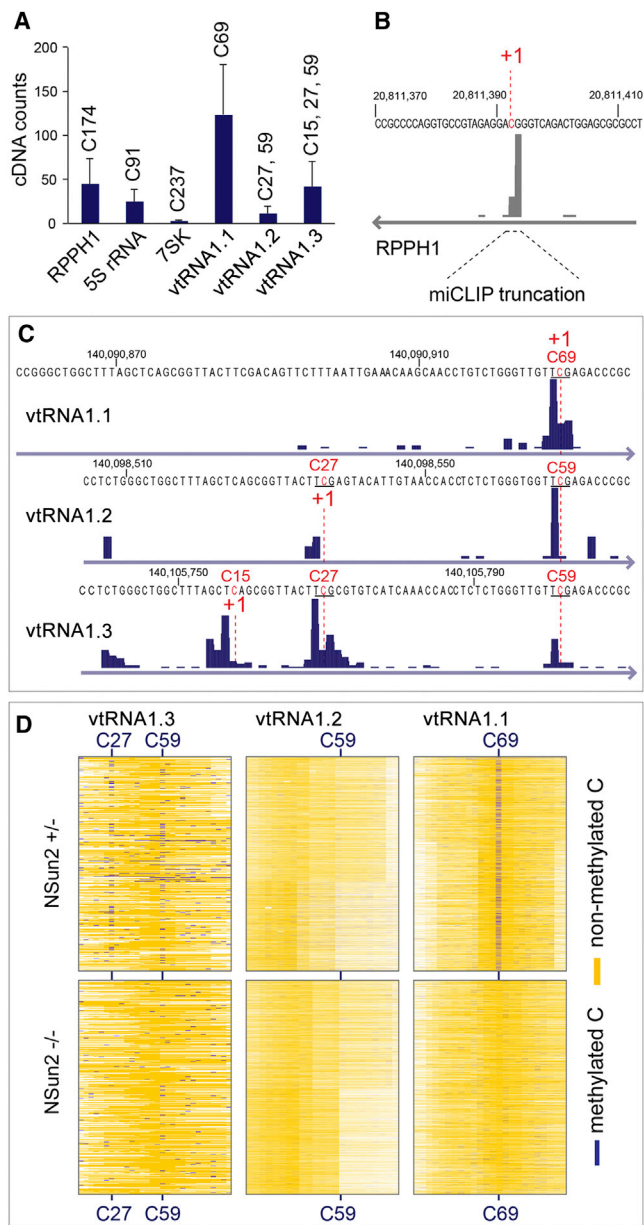


**Figure 3. Identification of m<sup>5</sup>C in Noncoding RNAs**  
 (A) Total number of cDNAs and position of the m<sup>5</sup>C modification mapping to RPPH1, 5S rRNA, 7SK, and vtRNA (vtRNA1.1, vtRNA1.2, vtRNA1.3) in three independent miCLIP experiments after 25 cycles of amplification. Error estimates represent SD of the mean.  
 (B and C) Detection of miCLIP sites mapped as a custom track on the UCSC genome browser in RPPH1 (B) and vtRNA1.1, vtRNA1.2, and vtRNA1.3 (C). +1 indicates the crosslinked cytosine. Underlined is the potential consensus site T(m<sup>5</sup>C)G.  
 (D) RNA bisulfite sequencing showing the total number of reads with methylated (blue) and nonmethylated (yellow) cytosines in vtRNA1.1, vtRNA1.2, and vtRNA1.3 in *NSUN2*<sup>+/-</sup> and *NSUN2*<sup>-/-</sup> human fibroblasts. See also Figure S4.

the surrounding sequence. T(m<sup>5</sup>C)G might act as a vtRNA-specific recognition site for processing factors. Human vtRNAs can be processed into small RNAs (svRNAs) by a mechanism

different from the canonical microRNA (miRNA) pathway, but at least some of these svRNAs can regulate gene expression similar to miRNAs (Persson et al., 2009). How the processing of vtRNAs into svRNAs is controlled was unknown, and we speculated that the deposition of m<sup>5</sup>C into vtRNA might determine its processing into svRNAs.

**Fragmentation of vtRNA into svRNAs Is Altered in the Absence of m<sup>5</sup>C**

To investigate whether methylation of the vtRNAs might affect their processing into svRNAs, we performed RNA sequencing of purified 15–35 nt fragments isolated from *NSUN2*<sup>+/-</sup> and *NSUN2*<sup>-/-</sup> human fibroblast. The sequence reads were aligned to vtRNAs, allowing no mismatch, and we only considered fragments with a total sum of 40 reads across four replicates in at least one of the conditions. We identified six vault ncRNA fragments, five of which mapped to vtRNA1.1 and one to vtRNA1.2 (Figure S6A).

Four out of the five fragments derived from vtRNA1.1 exhibited statistically significant (false discovery rate [FDR] < 0.05) differential abundances in *NSUN2*<sup>-/-</sup> and *NSUN2*<sup>+/-</sup> fibroblasts (Figures 4A and 4B). Only one of these fragments (svRNA4) was strongly reduced in the absence of NSun2, and its 5' start site precisely coincided with the NSun2-mediated methylation site at position C69 (Figures 4A and 4B). We confirmed differential abundances of svRNA1 and svRNA4 in *NSUN2*<sup>-/-</sup> cells by quantitative PCR (qPCR) (Figure 4C). To test whether the presence of svRNA4 depended on NSun2, we re-expressed full-length NSun2 (pB-NSun2) in *NSUN2*<sup>-/-</sup> fibroblasts via retroviral infection (Figure 4D; Figure S6B). The level of svRNA4 increased by more than 10-fold when NSun2 was re-expressed compared to control cells infected by an empty vector (pB-empty) (Figure 4E).

We speculated that m<sup>5</sup>C might affect processing of vtRNA1.1. Deposition of m<sup>5</sup>C at position 69 may induce the generation of svRNA4 by recruiting site-specific endonucleases. To test our hypothesis, we incubated synthetic vtRNA1.1 RNAs carrying or lacking m<sup>5</sup>C at position 69 with cell lysate from *NSUN2*<sup>-/-</sup> fibroblasts, to avoid methylation of the synthetic RNA, and measured the abundance of svRNA4 by qPCR (Figure 4F). The levels of svRNA4 were highest when vtRNA1.1 was methylated in two independent experiments (Figure 4F; Figure S6C).

svRNA4 shares a high sequence homology to vtRNA fragments bound to Argonaute (GACCCGCGGGCGCUCUCCAGU CCUUU) (Burroughs et al., 2011). We isolated small RNAs that copurified with Argonaute proteins in *NSUN2*<sup>+/-</sup> fibroblasts and confirmed that svRNA4 bound to both Argonaute 2 and Argonaute 3 (Figure 4G). Given that vtRNA fragments can repress gene expression similarly to miRNAs (Persson et al., 2009), we reasoned that svRNA4 might have miRNA-like functions. We computationally predicted potential svRNA4 target mRNAs (Kertesz et al., 2007) and selected the top 100 potential target mRNAs for further analysis (Table S7). Because the loss of NSun2 function causes neurodevelopmental disorders in humans, we focused on mRNAs related to human diseases (Abbasi-Moheb et al., 2012; Khan et al., 2012; Martinez et al., 2012). Potential target mRNAs included CACNG7 and CACNG8, both of which encode voltage-gated calcium channels (Burgess

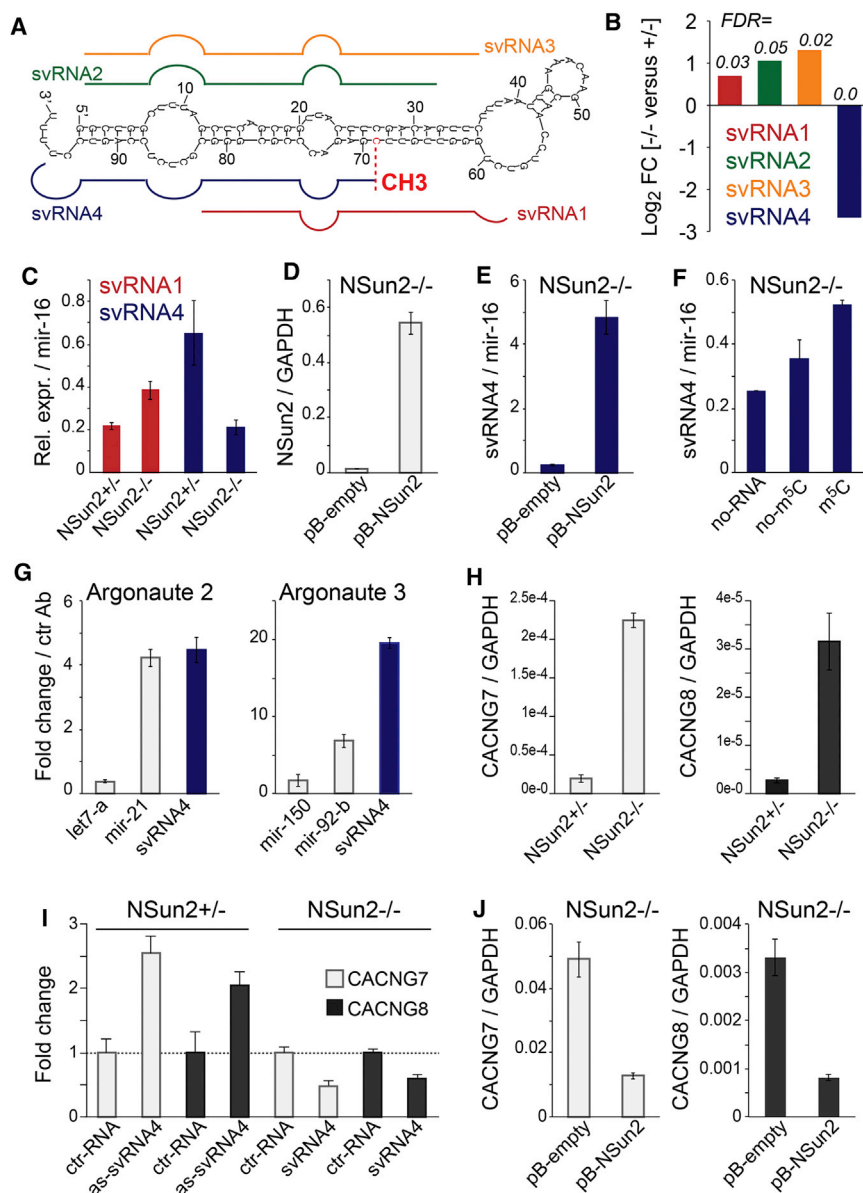


**Figure 4. Differential Processing of vtRNA1.1 into svRNAs in the Absence of m<sup>5</sup>C**

(A) Schematics of secondary structure of vtRNA1.1 and small vault RNA (svRNA) found to be differentially abundant in *NSUN2*<sup>+/-</sup> and *NSUN2*<sup>-/-</sup> fibroblasts. CH3, cytosine-5 methylated site at position 69.

(B) Fold-change (log<sub>2</sub>) and false discovery rate (FDR) values for reads of svRNA1-4 in *NSUN2*<sup>+/-</sup> versus *NSUN2*<sup>-/-</sup> human fibroblasts.

(C) Detection of svRNA1 and svRNA4 in *NSUN2*<sup>+/-</sup> and *NSUN2*<sup>-/-</sup> cells using qPCR. (D and E) RNA levels of NSun2 (D) and svRNA4 (E) in NSun2 null (-/-) fibroblasts rescued by viral infection of NSun2 (pB-NSun2) compared to the empty vector control (pB-empty).

(F) Abundance of svRNA4 in *NSUN2*<sup>-/-</sup> cell lysates (no-RNA) or incubated with synthetic vtRNA1.1 carrying (m<sup>5</sup>C) or lacking (no-m<sup>5</sup>C) at position 69.

(G) Detection of svRNA4 in small RNA pool copurified with Argonaute 2 (left) and Argonaute 3 (right). Let7-a and mir-150 are negative and mir-21 and mir-92-b are positive controls for Argonaute 2- and 3-bound microRNAs, respectively.

(H) qPCR showing expression of CACNG7 and CACNG8 RNA relative to GAPDH in *NSUN2*<sup>+/-</sup> and *NSUN2*<sup>-/-</sup> fibroblasts.

(I) Fold-change expression of CACNG7 and CACNG8 RNA in *NSUN2*<sup>-/-</sup> and *NSUN2*<sup>+/-</sup> fibroblasts transfected with svRNA4 microRNA mimics (svRNA4) versus respective control RNAs (ctr-RNA).

(J) RNA levels of CACNG7 and CACNG8 relative to GAPDH in NSun2 null (-/-) fibroblasts rescued by viral infection of NSun2 (pB-NSun2) compared to the empty vector control (pB-empty). Error estimates represent SEM (C-J). See also Figures S5 and S6.

et al., 2001; Waithe et al., 2011). Both CACNG7 and CACNG8 mRNA levels increased in *NSUN2*<sup>-/-</sup> fibroblasts, which was accompanied by increased CACNG8 protein levels (Figure 4H; Figure S6D).

To test whether svRNA4 exhibited miRNA-like functions, we transfected svRNA4 antagonists (as-svRNA4) and miRNA mimics (svRNA4) into *NSUN2*<sup>+/-</sup> and *NSUN2*<sup>-/-</sup> fibroblasts (Figure 4I). Inhibition of svRNA4 by its antagonist increased the levels of CACNG7 and CACNG8 mRNAs in *NSUN2*<sup>+/-</sup> fibroblasts, whereas transfection of svRNA4 mimics decreased mRNA levels in *NSUN2*<sup>-/-</sup> fibroblasts (Figure 4I). Finally, we confirmed that rescue of *NSUN2*<sup>-/-</sup> fibroblasts by overexpressing full-length NSun2 not only increased the levels of svRNA4 but also reduced the levels of CACNG7 and CACNG8 mRNAs and CACNG8 protein (Figures 4D, 4E, and 4J; Figures

4S6B, 4S6C, and 4S6E). Together, these results demonstrate that the loss of NSun2-mediated methylation of vtRNAs alters their processing into svRNAs and indicates that this affects the levels of svRNA-regulated mRNAs.

## DISCUSSION

Although the occurrence of methylated cytosine-5 was simultaneously discovered in DNA and RNA, the functional analysis of m<sup>5</sup>C in RNA was hampered by the lack of suitable technical tools. Bisulfite sequencing to chemically identify m<sup>5</sup>C in nucleosides was only recently adapted to RNA and confirmed site-specific methylation activity of NSun2 in tRNAs (Blanco et al., 2011; Martinez et al., 2012; Schaefer et al., 2009; Tuorto et al., 2012). System-wide RNA bisulfite sequencing confirmed NSun2-directed methylation of tRNAs and additionally identified C1NP and NAPRT1 mRNAs as well as the RNA subunit RPPH1 of

RNaseP as potential NSun2-methylated targets (Squires et al., 2012). The recent development of the Aza-IP method, a technique that exploits covalent bond formation between RNA methylases and the cytidine analogue 5-azacytidine, further identified SCARNA2 and vtRNA1.1 as bona fide target RNAs of NSun2 (Khoddami and Cairns, 2013). However, both RNA bisulfite conversion and Aza-IP rely on the chemical modification of the target RNAs, which may compromise RNA stability and integrity. Thus, the development of complementary methods to conclusively determine global NSun2-specific methylated transcriptomes was essential.

We have successfully used a mutated version of the NSun2 protein to induce the formation of an irreversible covalent cross-link between NSun2 and the methylated cytosine in its target RNA. Whereas miCLIP requires expression of the mutant NSun2 protein, it is independent of any chemical modification of nucleosides. We successfully mapped NSun2-specific binding to m<sup>5</sup>C in coding RNAs and ncRNAs. Our analysis identified around 300 common mRNAs among three replicates, indicating that NSun2-dependent methylation of coding RNAs is relatively rare. None of the miCLIP-identified mRNAs were differentially regulated in NSun2-depleted cells.

We confirmed vtRNAs as methylation substrates for NSun2 by RNA bisulfite sequencing using human skin fibroblast carrying a homozygous loss-of-function mutation in the *NSun2* gene (Martinez et al., 2012). vtRNAs are ncRNAs found as part of the vault ribonucleoprotein complex of unknown function (Kedersha and Rome, 1986). Interestingly, vtRNAs are significantly upregulated during neural differentiation (Skreka et al., 2012), and NSun2 deficiency in humans causes neurodevelopmental symptoms (Abbasi-Moheb et al., 2012; Khan et al., 2012; Martinez et al., 2012). However, the role of site-specific loss of m<sup>5</sup>C in vtRNAs in the NSun2-mediated functions remained unclear.

vtRNAs can be processed into regulatory small RNAs in a Dicer-dependent mechanism (Friedländer et al., 2012; Langenberger et al., 2013; Persson et al., 2009). Our study suggests that vtRNA methylation may add another layer of regulation to this process. We identified four differential abundant vtRNA-derived svRNAs in patient fibroblasts lacking the NSun2 protein, yet only one of those (svRNA4) decreased in the absence of NSun2. Our study suggests a mechanism whereby vtRNA methylation may act as a molecular switch to produce specific svRNAs, which in turn influence distinct sets of mRNAs. We identified CACNG7 and CACNG8 as potential mRNAs regulated via the vtRNA-derived small RNA svRNA4. In conclusion, our data indicate that NSun2-mediated m<sup>5</sup>C of vtRNAs regulates their processing into specific small RNAs and alterations in this pathway may contribute to symptoms found in humans with NSun2 deficiency.

## EXPERIMENTAL PROCEDURES

### miCLIP

Ethics approval was provided by the UCSD institutional review board. The Myc-tagged NSun2 C271A mutated construct (Hussain et al., 2009) or an empty vector control was transfected into COS7 or HEK293 cells using Lipofectamine 2000 (Invitrogen) and cells were harvested 24 hr later. NSun2 was immunoprecipitated with monoclonal Myc antibody (9E10), and iCLIP was subsequently performed as described before (König et al., 2010).

### Bisulfite Sequencing

Total RNA was extracted from human fibroblasts with TRIzol (Invitrogen), DNase (Ambion), and Ribo-zero treated (Epicenter, Illumina). The remaining RNA fraction was bisulfite-converted as previously described (Blanco et al., 2011). Bisulfite-converted libraries were generated according to the TruSeq Small RNA Preparation Kit (Illumina), after 3' and 5' ends were repaired with T4 PNK (New England Biolabs). RNA was then reverse transcribed followed by 18-cycle PCR amplification.

### Libraries for Deep Sequencing

For mRNA sequencing experiments, total RNA was obtained using TRIzol reagent (Invitrogen) and OligodT magnetic dynabeads were then used to isolate the mRNA fraction. For small RNA sequencing, total RNA from human fibroblasts was purified with the MirVana kit (Ambion) and then size-selected following separation on a 15% Novex TBE-Urea gel (Invitrogen). Libraries for sequencing were then prepared using the Illumina TruSeq Prep Kits and sequenced on the Illumina GAII platform.

### Real-Time qPCR

qPCR was performed using TaqMan assay sets purchased from Applied Biosystems or using the QuantifastSYBR green system (QIAGEN).

A detailed description of all experimental procedures is available in the Extended Experimental Procedures.

### ACCESSION NUMBERS

Sequencing data for cells derived from human patients have been deposited in the NIH Database of Genotypes and Phenotypes (dbGaP). The GEO accession number for the HEK293 sequencing data reported in this paper is GSE44386 (Table S8).

### SUPPLEMENTAL INFORMATION

Supplemental Information includes Extended Experimental Procedures, six figures, and eight tables and can be found with this article online at <http://dx.doi.org/10.1016/j.celrep.2013.06.029>.

### ACKNOWLEDGMENTS

We are most grateful to everyone who provided us with reagents. We thank the CI Genomics and Bioinformatics Core Facilities. We gratefully acknowledge the support of the Cambridge Stem Cell Initiative and Stephen Evans-Freke. This work was funded by Cancer Research UK, the Medical Research Council, and the European Research Council. Y.S. is supported by the Nakajima Foundation.

Received: February 19, 2013

Revised: May 20, 2013

Accepted: June 21, 2013

Published: July 18, 2013

### REFERENCES

- Abbasi-Moheb, L., Mertel, S., Gonsior, M., Nouri-Vahid, L., Kahrizi, K., Cirak, S., Wieczorek, D., Motazacker, M.M., Esmaeeli-Nieh, S., Cremer, K., et al. (2012). Mutations in NSUN2 cause autosomal-recessive intellectual disability. *Am. J. Hum. Genet.* 90, 847–855.
- Blanco, S., Kurowski, A., Nichols, J., Watt, F.M., Benitah, S.A., and Frye, M. (2011). The RNA-methyltransferase Misu (NSun2) poises epidermal stem cells to differentiate. *PLoS Genet.* 7, e1002403.
- Brzezicha, B., Schmidt, M., Makalowska, I., Jarmolowski, A., Pienkowska, J., and Szweykowska-Kulinska, Z. (2006). Identification of human tRNA:m<sup>5</sup>C methyltransferase catalysing intron-dependent m<sup>5</sup>C formation in the first position of the anticodon of the pre-tRNA Leu (CAA). *Nucleic Acids Res.* 34, 6034–6043.

- Burgess, D.L., Gefrides, L.A., Foreman, P.J., and Noebels, J.L. (2001). A cluster of three novel Ca<sup>2+</sup> channel gamma subunit genes on chromosome 19q13.4: evolution and expression profile of the gamma subunit gene family. *Genomics* 71, 339–350.
- Burroughs, A.M., Ando, Y., de Hoon, M.J., Tomaru, Y., Suzuki, H., Hayashizaki, Y., and Daub, C.O. (2011). Deep-sequencing of human Argonaute-associated small RNAs provides insight into miRNA sorting and reveals Argonaute association with RNA fragments of diverse origin. *RNA Biol.* 8, 158–177.
- Friedländer, M.R., Mackowiak, S.D., Li, N., Chen, W., and Rajewsky, N. (2012). miRDeep2 accurately identifies known and hundreds of novel microRNA genes in seven animal clades. *Nucleic Acids Res.* 40, 37–52.
- Goll, M.G., Kirpekar, F., Maggert, K.A., Yoder, J.A., Hsieh, C.L., Zhang, X., Golic, K.G., Jacobsen, S.E., and Bestor, T.H. (2006). Methylation of tRNAAsp by the DNA methyltransferase homolog Dnmt2. *Science* 311, 395–398.
- Hussain, S., Benavente, S.B., Nascimento, E., Dragoni, I., Kurowski, A., Gillich, A., Humphreys, P., and Frye, M. (2009). The nucleolar RNA methyltransferase Misu (NSun2) is required for mitotic spindle stability. *J. Cell Biol.* 186, 27–40.
- Hussain, S., Tuorto, F., Menon, S., Blanco, S., Cox, C., Flores, J.V., Watt, S., Kudo, N.R., Lyko, F., and Frye, M. (2013). The mouse cytosine-5 RNA methyltransferase NSun2 is a component of the chromatoid body and required for testis differentiation. *Mol. Cell Biol.* 33, 1561–1570.
- Kedersha, N.L., and Rome, L.H. (1986). Isolation and characterization of a novel ribonucleoprotein particle: large structures contain a single species of small RNA. *J. Cell Biol.* 103, 699–709.
- Kedersha, N.L., Miquel, M.C., Bittner, D., and Rome, L.H. (1990). Vaults. II. Ribonucleoprotein structures are highly conserved among higher and lower eukaryotes. *J. Cell Biol.* 110, 895–901.
- Kertesz, M., Iovino, N., Unnerstall, U., Gaul, U., and Segal, E. (2007). The role of site accessibility in microRNA target recognition. *Nat. Genet.* 39, 1278–1284.
- Khan, M.A., Rafiq, M.A., Noor, A., Hussain, S., Flores, J.V., Rupp, V., Vincent, A.K., Malli, R., Ali, G., Khan, F.S., et al. (2012). Mutation in NSUN2, which encodes an RNA methyltransferase, causes autosomal-recessive intellectual disability. *Am. J. Hum. Genet.* 90, 856–863.
- Khoddami, V., and Cairns, B.R. (2013). Identification of direct targets and modified bases of RNA cytosine methyltransferases. *Nat. Biotechnol.* 31, 458–464.
- King, M.Y., and Redman, K.L. (2002). RNA methyltransferases utilize two cysteine residues in the formation of 5-methylcytosine. *Biochemistry* 41, 11218–11225.
- König, J., Zarnack, K., Rot, G., Curk, T., Kayikci, M., Zupan, B., Turner, D.J., Luscombe, N.M., and Ule, J. (2010). iCLIP reveals the function of hnRNP particles in splicing at individual nucleotide resolution. *Nat. Struct. Mol. Biol.* 17, 909–915.
- Langenberger, D., Çakir, M.V., Hoffmann, S., and Stadler, P.F. (2013). Dicer-processed small RNAs: rules and exceptions. *J. Exp. Zool. B Mol. Dev. Evol.* 320, 35–46.
- Liu, Y., and Santi, D.V. (2000). m<sup>5</sup>C RNA and m<sup>5</sup>C DNA methyl transferases use different cysteine residues as catalysts. *Proc. Natl. Acad. Sci. USA* 97, 8263–8265.
- Martinez, F.J., Lee, J.H., Lee, J.E., Blanco, S., Nickerson, E., Gabriel, S., Frye, M., Al-Gazali, L., and Gleeson, J.G. (2012). Whole exome sequencing identifies a splicing mutation in NSUN2 as a cause of a Dubowitz-like syndrome. *J. Med. Genet.* 49, 380–385.
- Mossink, M.H., van Zon, A., Scheper, R.J., Sonneveld, P., and Wiemer, E.A. (2003). Vaults: a ribonucleoprotein particle involved in drug resistance? *Oncogene* 22, 7458–7467.
- Persson, H., Kvist, A., Vallon-Christersson, J., Medstrand, P., Borg, A., and Rovira, C. (2009). The non-coding RNA of the multidrug resistance-linked vault particle encodes multiple regulatory small RNAs. *Nat. Cell Biol.* 11, 1268–1271.
- Rai, K., Chidester, S., Zavala, C.V., Manos, E.J., James, S.R., Karpf, A.R., Jones, D.A., and Cairns, B.R. (2007). Dnmt2 functions in the cytoplasm to promote liver, brain, and retina development in zebrafish. *Genes Dev.* 21, 261–266.
- Redman, K.L. (2006). Assembly of protein-RNA complexes using natural RNA and mutant forms of an RNA cytosine methyltransferase. *Biomacromolecules* 7, 3321–3326.
- Schaefer, M., Pollex, T., Hanna, K., and Lyko, F. (2009). RNA cytosine methylation analysis by bisulfite sequencing. *Nucleic Acids Res.* 37, e12.
- Schaefer, M., Pollex, T., Hanna, K., Tuorto, F., Meusburger, M., Helm, M., and Lyko, F. (2010). RNA methylation by Dnmt2 protects transfer RNAs against stress-induced cleavage. *Genes Dev.* 24, 1590–1595.
- Skreka, K., Schaffner, S., Nat, I.R., Zywicki, M., Salti, A., Apostolova, G., Griehl, M., Rederstorff, M., Dechant, G., and Hüttenhofer, A. (2012). Identification of differentially expressed non-coding RNAs in embryonic stem cell neural differentiation. *Nucleic Acids Res.* 40, 6001–6015.
- Smith, C., Heyne, S., Richter, A.S., Will, S., and Backofen, R. (2010). Freiburg RNA Tools: a web server integrating INTARNA, EXPARNA and LOCARNA. *Nucleic Acids Res.* 38(Web Server issue), W373–7.
- Squires, J.E., Patel, H.R., Nusch, M., Sibbritt, T., Humphreys, D.T., Parker, B.J., Suter, C.M., and Preiss, T. (2012). Widespread occurrence of 5-methylcytosine in human coding and non-coding RNA. *Nucleic Acids Res.* 40, 5023–5033.
- Stadler, P.F., Chen, J.J., Hackermüller, J., Hoffmann, S., Horn, F., Khaitovich, P., Kretzschmar, A.K., Mosig, A., Prohaska, S.J., Qi, X., et al. (2009). Evolution of vault RNAs. *Mol. Biol. Evol.* 26, 1975–1991.
- Sugimoto, Y., König, J., Hussain, S., Zupan, B., Curk, T., Frye, M., and Ule, J. (2012). Analysis of CLIP and iCLIP methods for nucleotide-resolution studies of protein-RNA interactions. *Genome Biol.* 13, R67.
- Suzuki, M.M., and Bird, A. (2008). DNA methylation landscapes: provocative insights from epigenomics. *Nat. Rev. Genet.* 9, 465–476.
- Tuorto, F., Liebers, R., Musch, T., Schaefer, M., Hofmann, S., Kellner, S., Frye, M., Helm, M., Stoecklin, G., and Lyko, F. (2012). RNA cytosine methylation by Dnmt2 and NSun2 promotes tRNA stability and protein synthesis. *Nat. Struct. Mol. Biol.* 19, 900–905.
- Ule, J., Jensen, K.B., Ruggiu, M., Mele, A., Ule, A., and Darnell, R.B. (2003). CLIP identifies Nova-regulated RNA networks in the brain. *Science* 302, 1212–1215.
- Waihe, D., Ferron, L., and Dolphin, A.C. (2011). Stargazin-related protein  $\gamma_7$  is associated with signalling endosomes in superior cervical ganglion neurons and modulates neurite outgrowth. *J. Cell Sci.* 124, 2049–2057.
- Zhang, X., Liu, Z., Yi, J., Tang, H., Xing, J., Yu, M., Tong, T., Shang, Y., Gorospe, M., and Wang, W. (2012). The tRNA methyltransferase NSun2 stabilizes p16INK<sup>4</sup> mRNA by methylating the 3′-untranslated region of p16. *Nat. Commun.* 3, 712.